CORE
Metadata, citation and similar papers at core.ac.uk
Provided by DSpace at Rice University

NANO LETTERS
2004
Vol. 4, No. 12
2355−2359

Scattering Spectra of Single Gold Nanoshells

Colleen L. Nehl,[†] Nathaniel K. Grady,[‡] Glenn P. Goodrich,[‡] Felicia Tam,[†] Naomi J. Halas,[‡,§] and Jason H. Hafner*[,†,§]

Departments of Physics and Astronomy, Electrical and Computer Engineering, and Chemistry, Rice University, Houston, Texas 77005

Received August 27, 2004; Revised Manuscript Received October 8, 2004

ABSTRACT

Single particle dark field spectroscopy has been combined with high-resolution scanning electron and atomic force microscopy to study the scattering spectra of single gold/silica nanoshells. The plasmon resonant peak energies match those calculated by Mie theory based on the nanoshell geometry. The resonance line widths fit Mie theory without the inclusion of a size-dependent surface scattering term, which is often included to fit ensemble measurements. These results suggest that plasmon spectral measurements of nanoparticle ensembles are broadened due to particle inhomogeneity.

Noble metal nanoparticles exhibit particle plasmon resonances at optical frequencies, making them strong scatterers and absorbers of visible light with resonant peak wavelengths and line widths that are highly sensitive to the nanoparticle size, shape, and local environment.[1,2] These properties, coupled with recent advances in nanoparticle synthesis and assembly,[3] have stimulated interest in the use of plasmon resonant nanoparticles and nanostructures as biological and chemical sensors.[4] Plasmon resonances also allow for the manipulation and enhancement of local electromagnetic fields at nanoparticle surfaces, spurring applications in surface enhanced spectroscopies[5] and photonic devices.[6]

The spectral extinction of noble metal nanoparticles has been studied experimentally on nanoparticle ensembles and compared to Mie theory calculations with the complex dielectric function of the metal[7] included as an empirical parameter.[2] Mie theory accurately predicts the dipole and higher order plasmon resonant energies as a function of particle size and environment. However, the resonant line widths, which physically correspond to the coherence lifetime of the plasmon excitation, are underestimated by Mie theory for small particles (<20 nm diameter).[1,8−11] The observed line width broadening is typically explained by invoking a size-dependent modification of the bulk dielectric function to include contributions for surface scattering as the particle size becomes smaller than the electron mean free path. Inhomogeneous broadening due to varying particle size and shape, although difficult to assess, should also be considered[12] but is usually assumed to be unimportant. Recently, spectral scattering measurements have emerged which completely remove inhomogeneous broadening by studying a single nanoparticle.[13−21] In the case of spherical nanoparticles for which analytical Mie calculations are available,[14,16,21] these results suggest that the additional surface scattering term is not necessary. A recent report on the spectra of single Au/Au_2S nanoshells also suggests that electron surface scattering has reduced significance.[22] Here we report similar measurements on larger Au/silica nanoshells where phase retardation is significant.

Gold nanoshells are versatile nanophotonic particles whose plasmon resonance can be tuned from the visible through the infrared by adjusting the ratio of their core and shell radii.[23,24] They can be fabricated by the reduction of $HAuCl_4$ in an aged Na_2S solution,[25,26] or by the growth of thin metal films on silica colloids through molecular self-assembly and $HAuCl_4$ reduction.[27] Due to their spherical symmetry, nanoshell extinction spectra can be determined analytically by Mie theory,[23,28] which accurately predicts the positions and relative strengths of the dipole and higher order resonances as determined by extinction measurements on nanoshell solutions.[27,29,30] Their stable structure and tunable resonances have led to significant applications in drug delivery,[31] photothermal cancer therapy,[32,33] and surface-enhanced spectroscopy.[34]

For these experiments gold nanoshells were fabricated as previously described[27] to have a 60 nm radius silica core and a 20 nm thick shell. The measured (CARY 5000, Varian, Inc.) and calculated extinction spectra for an aqueous solution of these nanoshells are compared in Figure 1. The nanoshell Mie theory calculation[23,28] was carried out for a nanoshell with $r_1 = 60$ nm (the dielectric core) and $r_2 = 80$ nm (the total particle) in water ($n = 1.33$). Measured and calculated spectra in this and subsequent figures are normalized to have a peak value of 1. The calculated scattering and absorption

* Corresponding author. E-mail: hafner@rice.edu.
† Department of Physics and Astronomy.
‡ Department of Electrical and Computer Engineering.
§ Department of Chemistry.

10.1021/nl048610a CCC: $27.50 © 2004 American Chemical Society
Published on Web 11/04/2004

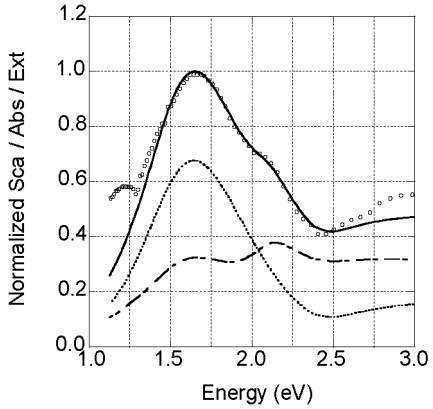

Figure 1. Measured extinction of an aqueous nanoshell suspension (circles) and calculated spectral extinction of gold nanoshells (line), both normalized. The Mie theory calculations were for a silica core radius of $r_1 = 60$ nm and an outer radius of $r_2 = 80$ nm with a scattering parameter $A = 1$. The measured nanoshell outer diameter is 160 nm (Figure 2). The calculated absorption (dashed) and scattering (dotted) components of extinction are also shown.

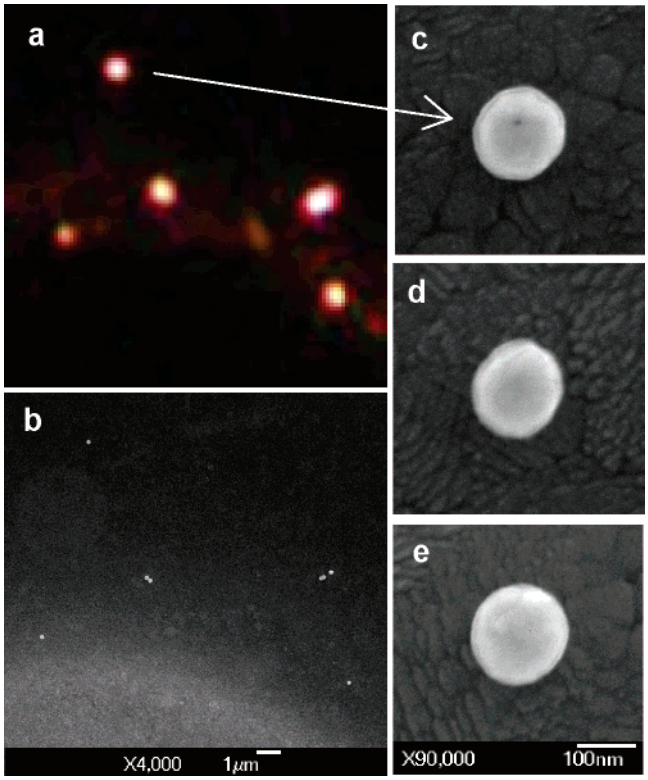

Figure 2. Optical (a) and SEM (b) images of nanoshells on ITO substrates relative to a gold reference mark. High-resolution SEM images (c−e) of three individual nanoshells are also shown.

components of the extinction are also shown. Scanning electron micrographs (SEM-5300, JEOL) of individual nanoshells (Figure 2) confirm that the outer radius is 80 nm. The excellent fit between the measured structure, extinction spectrum, and Mie theory calculation confirms the high quality of the nanoshell sample. To capture single-particle spectra, alignment marks were applied to indium tin oxide (ITO) coated glass slides ($R_S = 6 \pm 2\ \Omega$, Delta Technologies Limited), or plain glass slides, by evaporation of gold through enumerated transmission electron microscopy finder grids. Nanoshells were deposited onto these substrates by evaporation of a nanoshell suspension in ethanol. Optical imaging was carried out on an inverted microscope (Axiovert 200, Zeiss) with transmitted light dark field illumination (NA = 1 to 1.4) and an oil immersion objective (NA = 0.7). For optical characterization, nanoshells were either in immersion oil ($n = 1.5$) or water ($n = 1.33$) between the substrate and a coverslip. Under these conditions the nanoshells and edges of the alignment pattern are clearly visible against the dark background. Individual nanoshells observed in the optical microscope were characterized at high resolution (Figure 2) by scanning electron microscopy and atomic force microscopy (Bioscope, Veeco Metrology). To record a single-particle spectrum, the diffraction-limited image of a single nanoshell was placed at the entrance slit of an imaging spectrograph (SP-2156, Acton Research Corporation) and data were collected with a peltier-cooled CCD (Orca II ERG, Hamamatsu). A background spectrum, taken from a nearby position with no nanoshell image in the slit, was subtracted from the measured spectrum. The data were corrected for the spectral efficiency of the system by dividing by the spectrum of a white calibration standard (Edmund Industrial Optics).

Measured scattering spectra for the individual nanoshells imaged in Figure 2c−e are displayed in Figure 3a−c, as well as calculated nanoshell scattering spectra. We have found that concurrent optical and high-resolution structural characterization is critical for measuring single nanoparticle lineshapes. Single nanoshells and fused nanoshell dimers are clearly resolved in electron micrographs, but are indistinguishable in the optical microscope as demonstrated in Figure 4. The dimers have a broadened spectrum, which is likely an effect of plasmon hybridization[35] and does not reflect the homogeneous line width. The single nanoshell scattering spectra of Figure 3 retain the strong near-IR dipole resonance found in the bulk extinction spectrum, with peak wavelengths ranging from 1.6 to 1.7 eV. To match the measured peaks, r_1 and r_2 values were adjusted in the calculations by a few nanometers, with the shell thickness kept constant. The quadrupole peak is less prominent in the single-particle spectra than in the bulk extinction spectra. However, as demonstrated in Figure 1, the quadrupole signal is largely due to absorption, which is not measured in the single-particle spectrometer.

To achieve a more homogeneous dielectric medium and avoid possible complications due to the conductive ITO layer, single-particle spectra were also measured on glass substrates (no ITO) with the nanoshells in immersion oil (Figure 5). Since scanning electron microscopy cannot image insulating substrates, atomic force microscopy was employed to confirm that the nanoshells observed were indeed single. Note that in these data sets, the peaks are slightly red shifted relative to Figure 3, and that the quadrupole is more distinct. This is a result of the nanoshells being immersed in a medium of higher dielectric constant (immersion oil and glass, $n = 1.5$), thus increasing phase retardation effects.[2]

Mie theory calculations for metal nanoparticles include electronic structure through the complex dielectric function

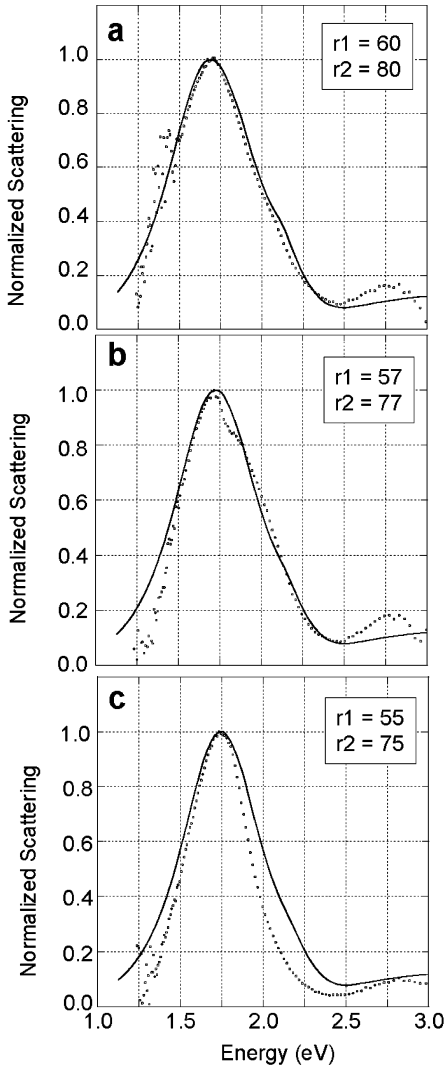

Figure 3. Measured scattering spectra for single nanoshells in water on ITO substrates (circles) and Mie theory calculations (lines). Spectra in a, b, and c correspond to the nanoshells in Figure 2 c, d, and e, respectively. The calculations were performed in a medium of $n = 1.33$ with no enhanced broadening ($A = 0$). The core and shell radii for each calculation are given in the figure.

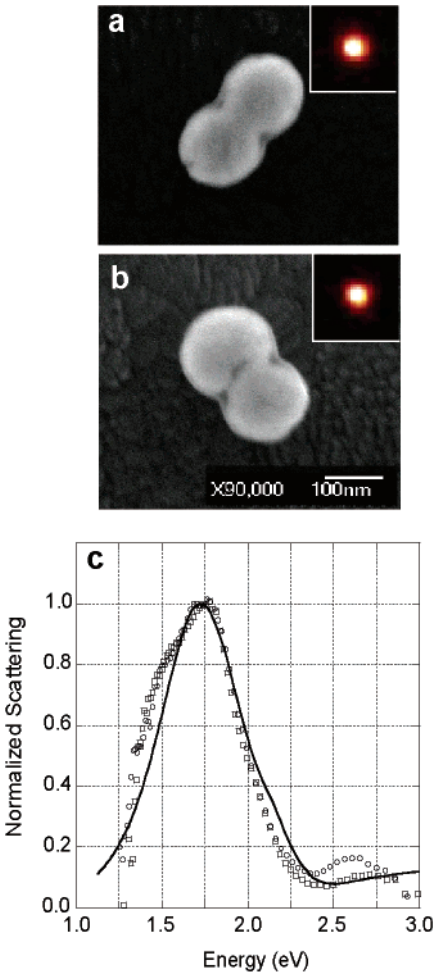

Figure 4. SEM images (a, b) of fused nanoshell dimers on ITO substrates. The insets are images from the dark field optical microscope of the same dimer particles. The magnifications and scale bars are all identical to Figure 2. The spectra of these two dimers (squares, circles) are plotted in c with the single nanoshell spectra calculation from Figure 3b (line) for reference.

of the bulk metal.[7] This empirical dielectric function can be fit by a model that includes an interband transition term and a Drude free electron term:

$$\epsilon(\omega) = \epsilon(\omega)_{\text{interband}} + \left(1 - \frac{{\omega_p}^2}{\omega^2 + i\omega\gamma_{\text{bulk}}}\right)_{\text{Drude}} \quad (1)$$

where ω is the frequency, ω_p is the bulk plasma frequency, and γ_{bulk} is the bulk scattering rate.[2,36] It is hypothesized that for particles that are small relative to the electron mean free path, γ_{bulk} is enhanced due to scattering at the particle boundary, thus requiring a modified scattering rate, Γ:

$$\Gamma = \gamma_{\text{bulk}} + A\frac{v_F}{a} \quad (2)$$

where v_F is the Fermi velocity, a is the reduced electron mean free path length due to the surface, and A is a parameter that depends on the details of the surface scattering process.[8−10] For spherical nanoparticles, a is simply related to the nanoparticle diameter. This modification of the bulk scattering rate reproduces the observed inverse relation between line width and nanoparticle size for small nanoparticles. The nanoshell extinction calculation in Figure 1 requires a surface scattering parameter of $A = 1$ to achieve a reasonable line width fit to the bulk nanoshell extinction measurement, consistent with previous results.[37] Although these nanoshells have an outer diameter larger than the electron mean free path in gold, it is the shell thickness that limits the electron path length and determines the amount of surface scattering. Therefore, a in eq 2 is set to the shell thickness for nanoshell calculations.[26,37]

The single nanoshell scattering spectra we observe have a significantly narrower line width than previously observed for gold ensemble nanoshell measurements in solution phase.[37] The full width at half-maximum (fwhm) of the scattering portion of the spectrum in Figure 1 is 760 meV, while the single nanoshell spectra in Figure 3 have an average

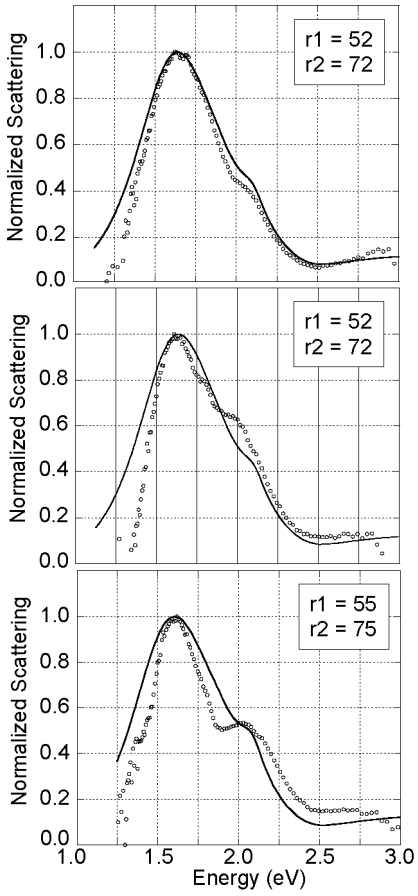

Figure 5. Measured scattering spectra for single nanoshells in immersion oil on glass substrates (circles) and Mie theory calculations (lines). Nanoshell singularity was confirmed by AFM. The calculations were performed in a medium of $n = 1.5$ with no enhanced broadening ($A = 0$). The core and shell radii for each calculation are given in the figure.

fwhm of 545 meV. The single nanoshell spectra in Figures 3 and 5 fit Mie theory calculations well with no surface scattering ($A = 0$). These results suggest that bulk nanoshell extinction spectra are indeed broadened by particle size and shape inhomogeneity, and that interfacial electron scattering does not contribute significantly to the observed ensemble line width. A full quantum description of nanoshell plasmon resonances using the time-dependent local density approximation (TDLDA) supports this view.[38] This calculation, which does not require the bulk dielectric function of gold as an input parameter, accurately predicts the dependence of the nanoshell plasmon resonant energy on the nanoshell structure, yet shows no dependence of the line width on the total diameter. A recent report on single Au/Au_2S nanoshells observed even narrower line widths, down to 180 meV, by studying smaller nanoshells (80 nm diameter) to reduce phase retardation effects that broaden the spectrum. When compared with Mie theory, the scattering parameter that best fit the data was $A = 0.5$, still smaller than values typically required to fit ensemble measurements.[22,37]

Note that the bottom spectra in Figures 3 and 5 have even smaller line widths than the Mie theory calculation with $A = 0$, as has been seen is some single-particle studies.[16,21] We believe that this deviation is real, since the vertical error bars are similar to the symbol sizes and the band-pass of the spectrometer is approximately 20 meV. The cause of this narrowing is currently under investigation. The particle-to-particle spectral variation in line width suggests that it may be related to surface roughness or defects in the nanoshell, which can impact the spectral properties.[39] Alternatively, this discrepancy may simply reflect a deviation of the nanoparticle dielectric function as compared to that of bulk gold.

In conclusion, we have measured the scattering spectra of single gold nanoshells by dark field microscopy. The spectral peak positions matched those of the bulk solution and were well fit by Mie theory without the need to invoke any additional homogeneous broadening mechanism, such as electron-surface scattering. This supports recent single-particle spectroscopy measurements that suggest that inhomogeneous broadening causes the increase in nanoparticle plasmon line width rather than surface scattering.[14,16,21] Nanoshells are an ideal particle for studying this issue. Like colloidal nanoparticles they are spherically symmetric and thus exactly solvable by Mie theory. However, with nanoshells, one can also independently adjust the relative line-width contributions of phase retardation (based on the total radius) and surface scattering (based on the shell thickness), as well as the dipole peak energy.

Acknowledgment. The authors gratefully acknowledge C. Oubre, P. Nordlander, and J. B. Jackson for helpful discussions, as well as support from the Laboratory for Nanophotonics at Rice University, the National Science Foundation (EEC-0304097), the Air Force Office of Scientific Research (F49620-02-1-0312), the Army Research Office (DAAD19-99-1-0314), NASA (68371), the Robert A. Welch Foundation (C-1220), and the NSF Center for Biological and Environmental Nanotechnology (EEC-0118007).

References

(1) Link, S.; El-Sayed, M. A. *Int. Rev. Phys. Chem.* **2000**, *19*, 409−453.
(2) Kreibig, U.; Vollmer, M. *Optical Properties of Metal Clusters*; Springer: Berlin, 1995.
(3) Tapan, S. K.; Murphy, C. J. *J. Am. Chem. Soc.* **2004**, *126*, 8648−8649.
(4) Haes, A. J.; Van Duyne, R. P. *J. Am. Chem. Soc.* **2002**, *124*, 10596−10604.
(5) Félidj, N.: Aubard, J.; Lévi, G.; Krenn, J. R.; Hohenau, A.; Schider, G.; Leitner, A.; Aussenegg, F. R. *Appl. Phys. Lett.* **2003**, *82*, 3095−3097.
(6) Maier, S. A.; Kik, P. G.; Atwater, H. A.; Meltzer, S.; Harel, E.; Koel, B. E.; Requicha, A. A. G. *Nat. Mater.* **2003**, *2*, 229−232.
(7) Johnson, P. B.; Christy, R. W. *Phys. Rev. B* **1972**, *6*, 4370−4379.
(8) Link, S.; El-Sayed, M. A. *J. Phys. Chem. B* **1999**, *103*, 8410−8426.
(9) Pinchuk, A.; Kreibig, U.; Hilger, A. *Surf. Sci.* **2004**, *557*, 269−280.
(10) Hövel, H.; Fritz, S.; Hilger, A.; Kreibig, U.; Vollmer, M. *Phys. Rev. B* **1993**, *48*, 18178−18188.
(11) Kraus, W. A.; Schatz, G. C. *J. Chem. Phys.* **1983**, *79*, 6130−6139.
(12) Vartanyan, T.; Simon, M.; Träger, F. *Appl. Phys. B* **1999**, *68*, 425−431.
(13) Michaels, A. M.; Jiang, J.; Brus, L. *J. Phys. Chem. B* **2000**, *104*, 11965−11971.
(14) Klar, T.; Perner, M.; Grosse, S.; von Plessen, G.; Spirkl, W.; Feldmann, J. *Phys. Rev. Lett.* **1998**, *80*, 4249−4252.
(15) Krenn, J. R.; Schider, G.; Rechberger, W.; Lamprecht, B.; Leitner, A.; Aussenegg, F. R.; Weeber, J. C. *Appl. Phys. Lett.* **2000**, *77*, 3379−3381.
(16) Sönnichsen, C.; Franzl, T.; Wilk, T.; von Plessen, G.; Feldmann, J. *New J. Phys.* **2002**, *4*, 93.1−93.8.

(17) Sönnichsen, C.; Franzl, T.; Wilk, T.; von Plessen, G.; Feldmann, J.; Wilson, O.; Mulvaney, P. *Phys. Rev. Lett.* **2002**, *88*, 7740201−7740204.
(18) Mock, J. J.; Barbic, M.; Smith, D. R.; Schultz, D. A.; Schultz, S. *J. Chem. Phys.* **2002**, *116*, 6755−6759.
(19) Mock, J. J.; Smith, D. R.; Schultz, S. *Nano Lett.* **2003**, *3*, 485−491.
(20) Lindfors, K.; Kalkbrenner, T.; Stoller, P.; Sandoghar, V. *Phys. Rev. Lett.* **2004**, *93*, 03740101−03740104.
(21) Liau, Y.-H.; Unterreiner, A. N.; Chang, Q.; Scherer, N. F. *J. Phys. Chem. B* **2001**, *105*, 2135−2142.
(22) Raschke, G.; Brogl, S.; Susha, A. S.; Rogach, A. L.; Klar, T. A.; Feldmann, J.; Fieres, B.; Petkov, N.; Bein, T.; Nichtl, A.; Kürzinger, K. *Nano Lett.* **2004**, *4*, 1853−1857.
(23) Aden, A. L.; Kerker, M. *J. Appl. Phys.* **1953**, *22*, 1242−1246.
(24) Neeves, A. E.; Birnboim, M. H. *J. Opt. Soc. Am. B* **1989**, *6*, 787−796.
(25) Zhou, H. S.; Honma, I.; Komiyama, H.; Haus, J. W. *Phys. Rev. B* **1994**, *50*, 12052−12056.
(26) Averitt, R. D.; Sarkar, D.; Halas, N. J. *Phys. Rev. Lett.* **1997**, *78*, 4217−4220.
(27) Oldenburg, S. J.; Averitt, R. D.; Westcott, S. L.; Halas, N. J. *Chem. Phys. Lett.* **1998**, *288*, 243−247.
(28) Bohren, C.; Huffman, D. R. *Absorption and Scattering of Light by Small Particles*; Wiley: New York, 1983.
(29) Oldenburg, S. J.; Hale, G. D.; Jackson, J. B.; Halas, N. J. *Appl. Phys. Lett.* **1999**, *75*, 1063−1065.
(30) Oldenburg, S. J.; Jackson, J. B.; Westcott, S. L.; Halas, N. J. *Appl. Phys. Lett.* **1999**, *75*, 2897−2899.
(31) Sershen, S. R.; Westcott, S. L.; Halas, N. J.; West, J. L. *J. Biomed. Mater. Res.* **2000**, *51*, 293−298.
(32) Hirsch, L. R.; Stafford, R. J.; Bankson, J. A.; Sershen, S. R.; Rivera, B.; Price, R. E.; Hazle, J. D.; Halas, N. J.; West, J. L. *Proc. Natl. Acad. Sci. U.S.A.* **2003**, *100*, 13549−13554.
(33) Loo, C.; Lin, A.; Hirsch, L. R.; Lee, M.-H.; Barton, J.; Halas, N. J.; West, J. L.; Drezek, R. A. *Technol. Cancer Res. Treat.* **2004**, *3*, 33−40.
(34) Jackson, J. B.; Westcott, S. L.; Hirsch, L. R.; West, J. L.; Halas, N. J. *Appl. Phys. Lett.* **2003**, *82*, 257−259.
(35) Prodan, E.; Radloff, C.; Halas, N. J.; Nordlander, P. *Science* **2003**, *302*, 419−422.
(36) Ashcroft, N. W.; Mermin, N. D. *Solid State Physics*; Saunders College: Philadelphia.
(37) Westcott, S. L.; Jackson, S. B.; Radloff, C.; Halas, N. J. *Phys. Rev. B* **2002**, *66*, 15543101−15543105.
(38) Prodan, E.; Nordlander, P. *Nano Lett.* **2003**, *3*, 543−547.
(39) Oubre, C.; Nordlander, P. *J. Phys. Chem. B* in press, 2004.

NL048610A